J Plant Dis Prot (2025) 132:48
https://doi.org/10.1007/s41348-024-01028-3

ORIGINAL ARTICLE

Transcriptional profiling of *Fraxinus excelsior* leaves during the early infection phase of ash dieback

Renata Callegari Ferrari[1,2] · Victor Chano[1,2] · Karuna Shrestha[1,6] · Tania Dominguez-Flores[1] · Maia Ridley[3,7] · Barbara Fussi[4] · Hannes Seidel[4] · Oliver Gailing[1,2] · Katharina B. Budde[1,5]

Received: 20 December 2023 / Accepted: 18 September 2024 / Published online: 21 December 2024

Abstract

Ash dieback (ADB) has been causing the progressive decline of *Fraxinus excelsior* trees throughout Europe, urging research and forest management to develop strategies to combat ADB. A genetically heritable component in susceptibility to this fungal disease was reported in common gardens. Thus, exploring the molecular basis of ADB susceptibility will further support breeding initiatives in the future. We performed transcriptional profiling of infected and uninfected leaves from two ash genotypes with different susceptibility to *Hymenoscyphus fraxineus*. Leaf rachises were sampled one week following inoculation. Differential gene expression analysis was performed to compare between treatments in each genotype (individual response) or in genotypes and treatments combined (common response). Due to the heterogeneity in the response, only DEGs were discussed that passed stringent assessment. Our results revealed that UW1, the most susceptible genotype, showed a total of 515 differentially expressed genes (DEGs), some of them possibly suggesting a self-control mechanism, hindering an effective immune response and causing increased susceptibility. On the other hand, FAR3, the least susceptible genotype with 230 DEGs, seemed to induce a contained but more efficient response, hinting toward a salicylic acid-mediated process and activating pathogen-related (like) proteins as thaumatin-like, peroxidases, and chitinases. In the common response, 512 DEGs were modulated and transcripts from the phenylpropanoid pathway were commonly altered in both genotypes. Altogether, this work comprised an initial transcriptional exploration including two selected genotypes with distinct susceptibility to ADB, however, the heterogenous response indicated the need to further improve the experimental inoculation approach. Exploring gene expression patterns in ADB susceptibility holds promise to reveal early response mechanisms, and new markers related to susceptibility, as well as to contribute to developing strategies that may help contain ADB.

Keywords *Fraxinus excelsior* · *Hymenoscyphus fraxineus* · Genotypes · Heritable susceptibility · RNA-seq

Introduction

Forest ecosystems shelter biodiversity and provide important ecosystem services such as the prevention of soil erosion, water regulation, and carbon storage (Thompson et al. 2011). However, higher demands for natural resources due to increases in human population, markets, worldwide trade, and transport in combination with climate change are strongly affecting forests. These factors have led to a loss of coverage and changes in the geographic distribution of the remaining forests (Ramsfield et al. 2016), and in this disrupted scenario, the transport and establishment of invasive

✉ Oliver Gailing
ogailin@gwdg.de

✉ Katharina B. Budde
katharina.budde@nw-fva.de

1 Department of Forest Genetics and Forest Tree Breeding, Faculty of Forest Sciences, University of Göttingen, Göttingen, Germany

2 Center for Integrated Breeding Research (CiBreed), University of Göttingen, Göttingen, Germany

3 Institute for Forest Protection, Julius Kühn-Institut, Brunswick, Germany

4 Bavarian Office for Forest Genetics (AWG), Teisendorf, Germany

5 Northwest German Forest Research Institute, Hann. Münden, Germany

6 Teagasc, Crops Research Centre, Oak Park, Carlow, Ireland

7 Institute of Forest Sciences, Albert-Ludwigs-University Freiburg, Freiburg, Germany

insect and pathogen species has been facilitated (Simler-Williamson et al. 2019). Thus, several cases of severe tree diseases are currently known, such as the Dutch elm disease, sudden oak death, chestnut blight, white pine blister rust, and the dieback of European common ash (Budde et al. 2016).

Ash dieback (ADB), a lethal fungal disease, has been severely reducing ash populations over the last 30 years (Pautasso et al. 2013). Throughout Europe, common ash (*Fraxinus excelsior* L.) trees are important not only for their centuries-long cultural and economic value (Bell et al. 2008; Pratt 2017), but also due to their fundamental ecological role for many associated species (Enderle et al. 2019). In terms of distribution, ash is a strong colonizer, but rarely becomes a dominant species (Heuertz et al. 2004a). The population genetic structure of ash trees indicates a high gene pool diversity with restricted genetic exchange between populations in southeastern Europe and in Sweden, while a widespread gene pool is prevalent in central and western European populations (Heuertz et al. 2004b). In regions where a scattered distribution leads to limited gene flow between different locations, the species is considered potentially vulnerable to genetic erosion (Myking 2002; Heuertz et al. 2004a).

The first cases attributed to ADB were reported in the early 1990s in Poland, involving a high mortality of ash trees regardless of age (Kowalski 2006). Later, the ascomycete *Hymenoscyphus fraxineus* (previously named *Chalara fraxinea* and *Hymenoscyphus pseudoalbidus* for its asexual and sexual stages, respectively) was identified to be the causal agent (Baral et al. 2014). The disease cycle starts between June and September, when ascospores penetrate the leaf surface via appressoria, resulting in necrotic spots and, sometimes, leading to leaf shedding approximately 10–14 days later (Kräutler and Kirisits 2012; Cleary et al. 2013). In fall, black pseudosclerotia develop in petioles and leaf rachises in the litter from which white-stalked apothecia will develop during the following warm season and release new ascospores (Gross and Holdenrieder 2013; Timmermann et al. 2011). The infection leads to death in most ash trees and has spread over entire countries. In association with the decline of other tree species in flood plain forests, such as elms due to Dutch elm disease or alder and pedunculate oak due to various *Phytophthora* species (Pautasso et al. 2013), ADB now represents a major threat to European biodiversity.

Susceptibility to ADB is a polygenic and moderately heritable trait. Ash trees infected with *H. fraxineus* show genetically controlled responses, such as early flushing of the buds or early shedding of leaves in autumn, which have been correlated with ash dieback susceptibility (McKinney et al. 2011; Muñoz et al. 2016). Furthermore, when comparing damaged crowns of clones grown in different locations, a single genotype is usually affected to a similar degree regardless of the environment (McKinney et al. 2012). Overall, as reviewed in Enderle et al. (2019), several studies from progeny and clonal field trials reported narrow-sense (ranging from 0.37 to 0.53) and broad-sense heritability values (ranging from 0.10 to 0.65), corroborating a moderate genetic control of ADB susceptibility.

In this context, further research efforts to understand the mechanisms underlying susceptibility to ADB and to develop suitable conservation, forest management, and breeding programs are of utmost importance and have been considered a measure to deal with the ash dieback epidemic (Pautasso et al. 2013; Enderle et al. 2019). One key and cost-effective strategy to investigate biological systems is to study transcriptional modulations as a means to explore gene expression in response to biotic stressors (Wang et al. 2009). More specifically, this approach can lead to the identification of genes involved in the response to a pathogen attack, allowing the development of genetic markers for breeding programs (Müller et al. 2023). Still, the molecular basis of ADB susceptibility and its mechanisms have not been exhaustively studied, and the exploration of the transcriptional response to ADB is currently very limited, even though reference genomes of common ash are already available (Sollars et al. 2017; Meger et al. 2024). As examples, tissue colonization assessed by pathogen transcript monitoring following rachis inoculation in common (*F. excelsior*) and Manchurian ash trees (*F. mandschurica* Rupr.) have reinforced a correlation between field performance and the infection intensity, and also highlighted a role for the timing of metabolic response during the infection process (Nielsen et al. 2022). In a transcriptional profiling study of border regions of necrotic spots on ash bark 10 months after infection, it was possible to identify that the mevalonate and iridoid pathways are modulated following infection, also revealing modulated transcription factors (TFs) and genes that are part of the jasmonate signaling pathway (Sahraei et al. 2020). Moreover, a metabolite expression study on ash bark tissue revealed the two coumarins, fraxetin and esculetin, to be strongly associated with susceptibility (Nemesio-Gorriz et al. 2020).

To contribute to the future preservation and management of ash trees, the research network FraxForFuture was formed in Germany in 2020 (Langer et al. 2022). The current work is a part of the FraxGen subproject, and we focused on performing an initial RNA-Seq analysis of genotypes with different susceptibility to ash dieback, which were sampled during the early infection phase. Our work with mock-inoculated and pathogen-inoculated ash trees indicated that significant transcriptional changes could be detected already seven days after inoculation. Moreover, we compared lists of differentially expressed genes (DEGs) which were significantly modulated between control and infected groups for each genotype individually, also identifying commonly regulated DEGs in both genotypes. Overall, our aim was to start laying a foundation for transcriptomic studies on infected ash leaves under controlled conditions and, although we observed experimental variability, we reinforce the potential of transcriptionally investigating ash genotypes differing in susceptibility. This strategy will allow for the identification of genomic variants in candidate genes that could be used for marker-assisted selection and contribute to the development of new breeding strategies and conservation initiatives.

Material and methods

Plant material, growth conditions, experimental setup and data acquisition

The plant material was provided by the Bavarian Agency of Forest Genetics (Bayrisches Amt für Waldgenetik, AWG). European ash trees growing in a clonal garden in Grabenstätt have been monitored since 2014. At the time the adult trees were selected in the field (2010) they were all identified as less susceptible (Fig. 1). The two clones selected for this study (FAR3, UW1) were within the first third of less susceptible clones using long-term crown damage inspection. The FAR3 clone was identified as the least susceptible and the clone UW1 as susceptible, ranging in the middle compared to all other 35 clones within the trial (Seidel et al. in prep.; Fig. 1). The most susceptible and heavily affected genotypes could not provide a sufficient amount of scions for grafting, justifying the choice of UW1 instead. FAR3 was originally collected close to the town Haiming at approximately 48.21°N, 12.90°E, and UW1 was collected close to the town Unterwössen at approximately 47.72°N, 12.46°E.

Scions were cut in winter 2020/2021 and replicated by grafting in February 2021 onto 2-year-old *F. excelsior* trees as rootstocks. The ash trees used as rootstocks came from a nursery, provided by Erwin Vogt Baumschulen GmbH, Pinneberg, the provenance was north-west Germany, code 81,101. Plants were grown in 4 L plastic pots containing a commercially available substrate mixture "Profi-Linie mineralisch" from Kleeschulte Erden GmbH & Co. KG, Rüthen, with pH ($CaCl_2$) 6.0, Salinity 1.5 g/L, N 320 mg/L, P_2O_5 120 mg/L, K_2O 350 mg/L, Mg: 120 mg/L. Six grafted trees per genotype were kept in a greenhouse with natural light conditions and semi-controlled humidity and temperature (Fig. 2A). Plants were repotted, fertilized, and watered regularly. The current experiment reported here was conducted in July 2021.

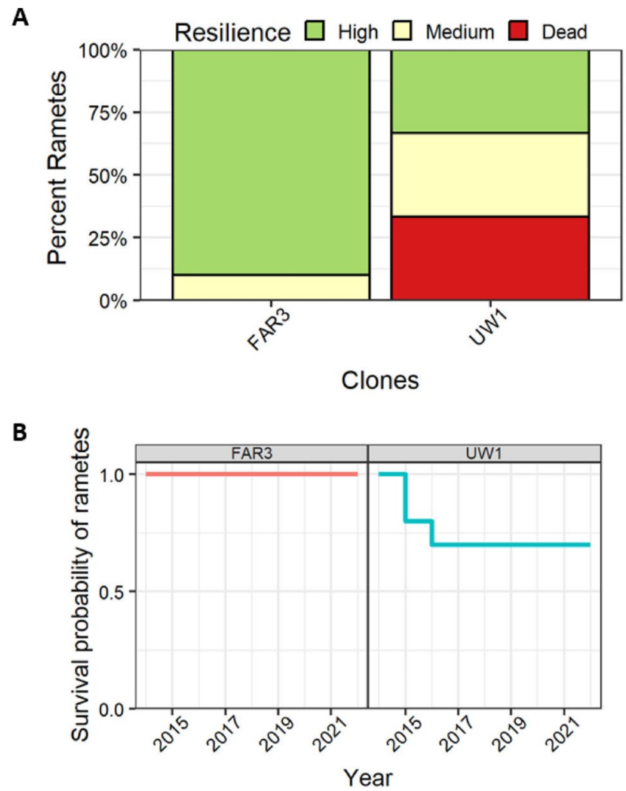

Fig. 1 European ash trees monitored since 2014 in a clonal common garden in Grabenstätt, in which the clone FAR3 was identified as the least susceptible and the clone UW1 as susceptible. **A** Percent of tree mortality for the two genotypes used in the present study. **B** Survival probability rate of ramets during the years of monitoring (Seidel et al. in prep.)

Pathogen inoculation and sampling

Isolates of *H. fraxineus* were tested for virulence and maintained in the culture collection at Julius Kuehn Institute (JKI), Federal Research Centre for Cultivated Plants, Institute for Forest Protection, Braunschweig, Germany. The most virulent strain (Strain 7—RH03-T2-B1-1) was selected as the reference strain based on severe symptom development after stem and petiole inoculations in saplings (Ridley et al. 2024). The *H. fraxineus* reference strain culture has been deposited in the DSMZ (German Collection of Microorganisms and Cell Cultures, Braunschweig, Germany) as DSM 116307.

The reference strain was cultivated at room temperature for approximately three weeks on MYP medium (prepared by mixing 2.8 g malt, 0.4 g peptone, 0.2 g yeast, 6 g agar, 400 ml ultrapure water, and circa 5 g ash leaves). Autoclaved wooden toothpicks (approx. 0.5 cm) were cultivated together with the pathogen for two weeks and used for inoculation (Fig. 2B, C). Toothpicks were placed inside a 1 cm-long superficial wound in the rachis (for a

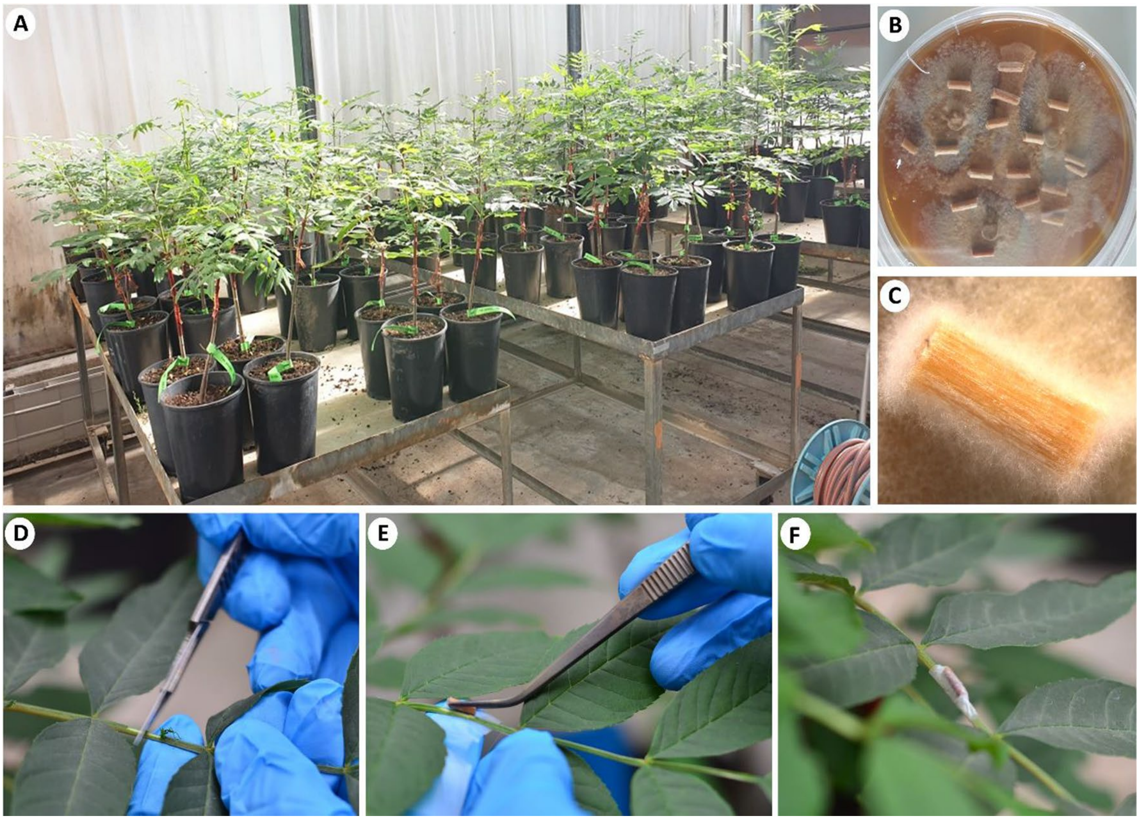

Fig. 2 Schematic of the experimental inoculation procedure. **A** Greenhouse with potted *Fraxinus excelsior* trees, which were grafted from scions originating from individuals with different susceptibility to ash dieback disease. **B** Culture plates of *Hymenoscyphus fraxineus* strain 7—RH03-T2-B1-1. **C** Wooden stick covered with *H. fraxineus*. **D** A 1 cm superficial wound on the rachis of ash leaves was cut with a scalpel. **E** A wooden stick was placed on the wound. **F** Sealing of the wound by wrapping the wooden stick with parafilm

morphological reference of the leaf regions, see Nielsen et al. 2022) (Fig. 2D) and sealed with parafilm (Fig. 2E). Autoclaved toothpicks incubated on sterile medium were used as controls. Collection of leaf samples took place after seven days following the inoculation, although there were no clear signs of necrosis development yet. The rachis region comprising the wound, in addition to 1 cm distally and proximally, respectively, from the inoculation wound were flash-frozen in liquid N_2 and kept at −60 °C until further use. Three biological replicates for each genotype were sampled.

RNA isolation and sequencing

For each sample 40–60 mg of rachis tissue were ground without thawing using a Retsch MM300 (F. Kurt Retsch, Haan, Germany). RNA was extracted using the E.Z.N.A. Plant RNA Kit Omega Bio Tek (R6827-01, Norcross Georgia, USA) according to the manufacturer's protocol for difficult samples. The concentration and purity of the RNA were assessed using a microvolume spectrophotometer (NanoDrop 2000, Thermo Fisher Scientific, Waltham, United States), and values between 1.8 and 2.2 for $A_{260/280}$ nm and $A_{260/230}$ ratios were considered sufficiently pure. In case these ratios were slightly lower than the optimal, a precipitation protocol was performed, involving overnight incubation at −20 °C with absolute ethanol, followed by centrifugation at 4 °C, two consecutive washes with 70% ethanol and centrifugation at room temperature, and resuspension with nuclease-free water.

Total RNA samples were treated with DNase I (Thermo Scientific) and the RNA quality was assessed using a Fragment Analyzer System (PROSize 3.0, 3.0.1.5, 2015, Advanced Analytical Technologies, Agilent Technologies). cDNA libraries were prepared with the Stranded mRNA Prep kit (Illumina, San Diego, USA), which uses oligo(dT) magnetic beads for purifying and capturing polyA tails from mRNA molecules. Libraries were sequenced using the Illumina HiSeq4000 platform, 50 bp and single-end reads.

Bioinformatic processing and differential gene expression analysis

The bioinformatic analyses were carried out in a High-Performance Computing (HPC) Center from the Gesellschaft für Wissenschaftliche Datenverarbeitung mbH Göttingen (GWDG), which is based on GNU/Linux and scheduled by Simple Linux Utility for Resource Management (SLURM; Yoo et al. 2003).

FastQC (v0.11.7), MultiQC (v.1.10.1) (Ewels et al. 2016), and Trimmomatic (v0.36) (Bolger et al. 2014) were used for quality control, removing adapter sequences, and trimming of 12 nucleotides from the head and 2 nucleotides from the tail of all reads. Reads shorter than 20 nucleotides and presenting an average quality score below 15 within a sliding window of 4 bases were filtered out. Subsequently, we used Hisat2 v.2.1.0 (Kim et al. 2019) to map fastq files to the *F. excelsior* reference genome version FRAX_001_PL (downloaded from https://www.ncbi.nlm.nih.gov/datasets/genome/ GCA_019097785.1/, Meger et al. 2024). Mapping was performed with the option –score-min L,0,-0.2, and mapped files were processed using Samtools v.1.9 (Li et al. 2009). Finally, counting was performed with HTSeq (v.2.0.2; Anders et al. 2015), using the GFF3 file obtained from the FRAX_001_PL version of the genome to indicate positions of mRNA in the genome (Meger et al. 2024). The final count-table was imported to R (R Core Team 2022) for downstream analysis.

The R package DESeq2 (Love et al. 2014) was employed to perform differential expression analysis. DESeq2 uses a Wald test to assess significance of negative-binomially distributed RNA-Seq data, with *P* values adjusted by the false discovery rate (FDR; Benjamini and Hochberg 1995). It also uses logarithmic fold change (LFC) values, which were defined as the logarithm of the ratio between treated (infected in this case) and untreated (control) samples. Expression values were first normalized using the variance stabilizing transformation (vst) method implemented in DESeq2, and transformed data were examined using a principal component analysis (PCA). Two approaches were used for expression analysis:

1. The "individual response" for each genotype was assessed comparing infected and control plants. Those transcripts with an adjusted *P* value below the standard 0.05 and showing a $\log_2$ fold change (LFC) >|1| were considered as Differentially Expressed Genes (DEGs). Volcano plots of the individual responses were generated with the R package EnhancedVolcano v.1.14 (Blighe et al. 2018). The two sets of DEGs obtained for each genotype were compared using a Venn diagram plotted with the R package ggVennDiagram v.1.2.2 (Gao et al. 2021).
2. The "common response" was analyzed by including the genotype factor as another variable in the DESeq2 formula design (see section Availability of Data and Code). DEGs were considered significant for adjusted *P* value < 0.05 and LFC >|1| for at least one of the genotypes. The results were visualized in a heatmap of the z-scores (calculated as the ratio between the mean and the standard deviation of each DEG) generated with the R package pheatmap v.1.0.12 (Kolde 2019).

We selected and discussed in particular genes with LFC >|2| and adjusted *P* value < 0.01 that were involved in immune responses, phenylpropanoid biosynthesis, mevalonate pathway, jasmonic acid (JA), salicylic acid (SA), and ethylene (ET) signaling pathways, as well as transcription factors (TFs) (Zamora-Ballesteros et al. 2021; Islam et al. 2022).

Functional annotation of DEGs, enrichment analysis, and gene selection

For the functional annotation of DEGs, we created a local protein database from the RefSeq Viridiplantae section at the National Center of Biotechnology Information (NCBI). A total of 41,355 gene model sequences from the genome version FRAX_001_PL were used (Meger et al. 2024) and included in a multi-fasta file used as input for BLASTp (Camacho et al. 2008). A maximum number of 50 hits per sequence was set, with an *e* value threshold of $10e^{-5}$, and results were imported into Omicsbox v3.0.30 (Götz et al. 2008) to complete the annotation with the Functional Analysis module. Annotation with GO terms encompassed the Mapping, Annotation, and GO-Slim steps, in addition to InterProScan which also retrieves GOs associated with protein motifs and domains. Functional annotation of the 41,355 gene models developed for the reference ash genome (FRAX_001_PL) resulted in 41,032 annotated transcripts (99.22%), while only 323 sequences (0.78%) could not be annotated for either Blast Hits, GO Mapping, GO Annotation or GO-Slim (Table 1). The complete annotation is shown in Supplementary Table 2.

Enriched GOs were identified by a two-tailed simple enrichment analysis (SEA) performed for all DEGs (the two individual responses for FAR3 and UW1, and the common response). The significance assessment was carried

Table 1 Overview of annotated sequences for gene models included in *Fraxinus excelsior* reference genome FRAX_001_PL

Annotation steps	Number of sequences
Total	41,355
Not annotated	323
Only with Blast Hits	495
Only with GO Mapping	7997
Only with GO Annotation	6552
With GO-Slim	25988

out, following Fisher's exact test featured by Omicxbox (Al-Shahrour et al. 2004), and using as reference the complete annotation in GO terms for all gene models.

Results

Ash genotypes could be clearly distinguished via transcriptome sequencing

An average of 32 million reads were generated for each sample (Supplementary Table 1). After trimming of low-quality transcripts and removal of contaminants, an average of approx. 31 million reads per sample were kept and from those, an average of 89.83% were mapped against the reference genome assembly FRAX_001_PL of *F. excelsior*. Total transcripts after quality filtering were used in a principal component analysis (Fig. 3). The first two principal components (PCs 1 and 2) explained 46% and 31% of the variance observed, respectively, and the genotypes UW1 and FAR3 could be easily distinguished along PC1. Biological replicates for the control group also showed a high conformance in PC2, whereas replicates for the pathogen-inoculated treatments showed a scattered distribution.

DEGs revealed distinct patterns of modulation between genotypes

After processing and annotation of sequenced reads, we performed separate differential gene expression analyses: the first to individually compare the modulations occurring in genotypes UW1 (higher susceptibility) and FAR3 (lower susceptibility), and second, the two genotypes jointly. This two-step approach sought to monitor DEGs in response to infection either in each individual genotype, or commonly modulated in both genotypes (see Methods section).

Figure 4a, b shows a graphical representation of the significant DEGs (adjusted *P* value < 0.05; LFC > |1|) in a comparison between control and treatment for each genotype. Patterns differ considerably, with a wider distribution of DEGs for UW1 (Fig. 4b). While a total of 230 DEGs were significantly modulated in FAR3, 515 were found in UW1. Among those, 136 were up- and 94 down-regulated in FAR3, whereas 444 were up- and 71 were down-regulated in UW1. The complete lists of identified DEGs for both genotypes and their respective LFC values and adjusted *P* values are provided in Supplementary Tables 3 and 4.

We compared the DEGs identified in each genotype and only nine genes were common between FAR3 and UW1, representing 1.2% of the total DEG number (Fig. 4c, Supplementary Table 5). These common genes included three WRKY transcription factors (TFs) (gene12571, gene14628, gene23853), an 1B-like ethylene-responsive TF (gene46078), a glucan endo-1,3-beta-glucosidase (gene41383), an alpha carbonic anhydrase (gene47080), a chloroplastic polyphenol oxidase I (gene51554), a 47 kDa synapse-associated protein (gene56171), and a suppressor of disruption of TFIIS (gene52496).

From the lists of DEGs for each genotype (Supplementary Tables 3 and 4), we selected and discussed in particular genes with LFC > |2| that were involved in immune responses, such as phenylpropanoid biosynthesis, mevalonate pathway, jasmonic acid (JA), salicylic acid (SA), and ethylene (ET) signaling pathways, and transcription factors (TFs) (Table 2). Most significant DEGs were up-regulated, but UW1 showed more down-regulated DEGs (34) than FAR3 (21). In the immune response category, FAR3 showed only thaumatin-like proteins and basic endochitinase-like, whereas UW1 also had several E3 ubiquitin-protein ligase proteins and a disease resistance response protein 206-like. In terms of secondary metabolites, although a similar number of DEGs was found for both genotypes in the category biosynthesis of phenylpropanoids, UW1 exclusively showed a 3-hydroxy-3-methylglutaryl-coenzyme A reductase 1-like from the mevalonate pathway, as well as a putative 12-oxo-phytodienoate reductase 11 as part of JA pathway. Numerous transcripts with varied functions in ET pathway were also up-regulated in UW1 (Table 2). Lastly, all five identified TFs in FAR3 were WRKYs, while for UW1 a diverse repertoire of TFs showed LFC > −2 (Table 2).

Separating the DEGs in up- and down-regulated sets per genotype did not yield any significantly enriched GO terms (results not shown). Therefore, we used the two full sets of DEGs (from FAR3 and UW1;

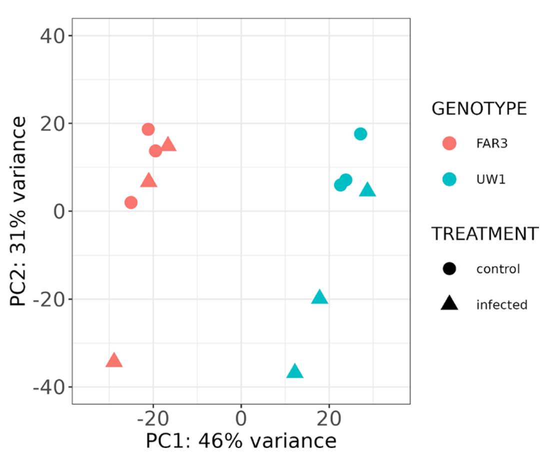

Fig. 3 Principal component analysis (PCA) of transcripts for the two genotypes of European ash (*Fraxinus excelsior*) showing higher (UW1) and lower (FAR3) susceptibility to ash dieback disease. Rachises were inoculated with the pathogen using wood plugs and allowed to grow for a week, when sampling of control (solid circles) and infected (solid triangles) groups occurred. Different colors indicate different genotypes and treatments

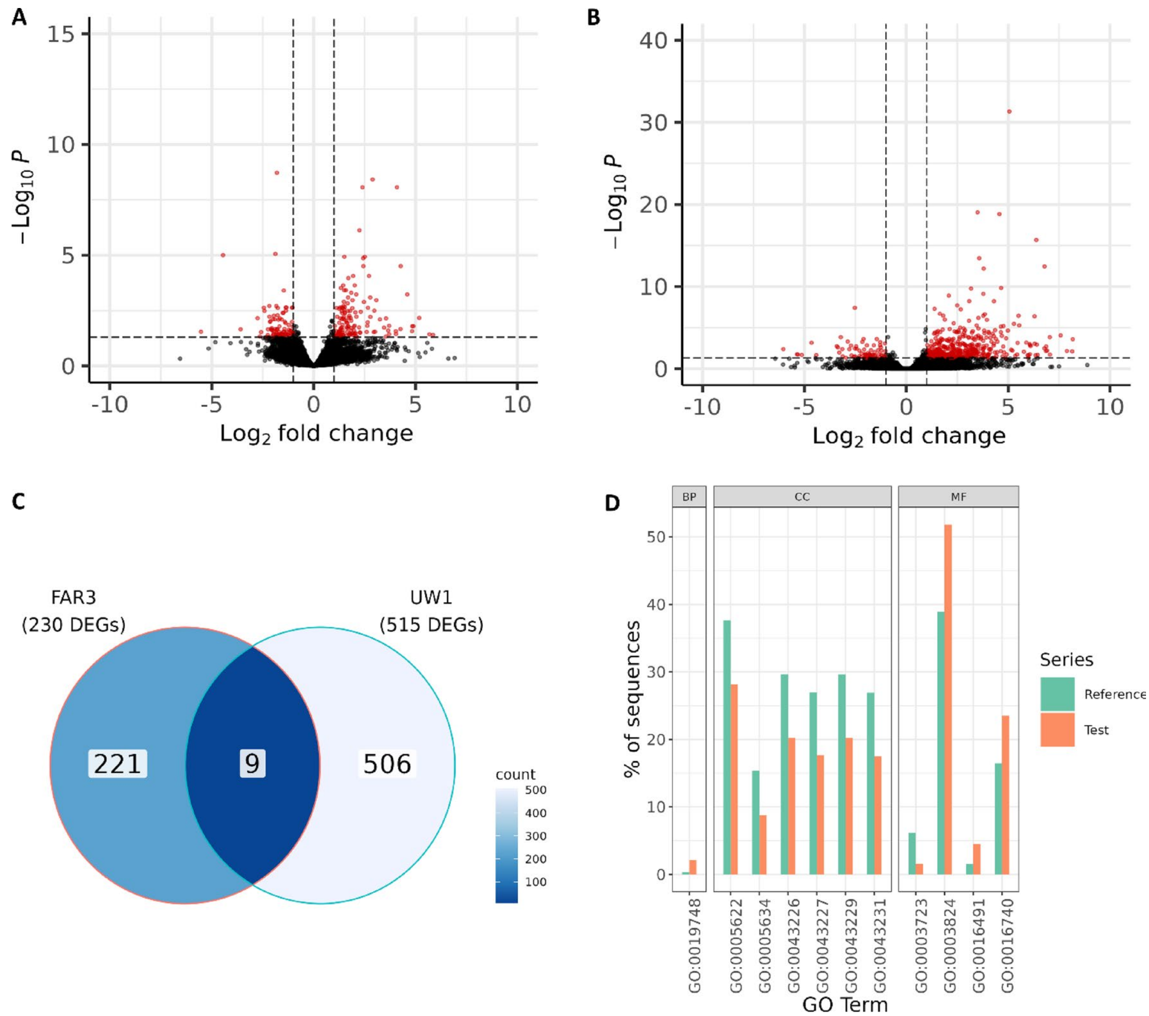

Fig. 4 Differential gene expression of two European ash genotypes that are more (UW1) or less (FAR3) susceptible to ash dieback. Leaf rachises of trees were inoculated with sterile or infected wood plugs and sampled after seven days. **A, B** Volcano plots for FAR3 (A) and UW1 (B). X-axis indicates $\log_2$-fold change values; y-axis indicates the $-\log_{10}$ of *P* values. Red circles indicate genes with adjusted *P* values of <0.05 and LFC $>|1|$. **C** Venn diagram of differentially expressed genes (DEGs) which are up- or down-regulated with adjusted *P* values of <0.05 and LFC $>|1|$. Blue color scale indicates the number of DEGs. **D** Enriched GO terms revealed after simple enrichment analysis (SEA) using the list of DEGs for UW1. Over-represented GOs are those with a higher percentage of sequences in the test (list of DEGs) than in the reference (complete list of gene models), while the percentage of sequences in under-represented GOs is higher in the Reference set. The description for the highlighted GO terms is as follows: GO:0019748 secondary metabolic process; GO:0005622 intracellular anatomical structure; GO:0005634 nucleus; GO:0043226 organelle; GO:0043227 membrane-bounded organelle; GO:0043229 intracellular organelle; GO:0043231 intracellular membrane-bounded organelle; GO:0003723 RNA binding; GO:0003824 catalytic activity; GO:0016491oxidoreductase activity; GO:0016740 transferase activity. The SEA results for FAR3 were not significant and are therefore not shown. *BP* biological process; *CC* cellular component; *MF* molecular function; *GO* Gene Ontology

Supplementary tables 3 and 4) to perform a two-tailed SEA of GO terms. While no significantly enriched GO terms were identified for FAR3 (Supplementary Table 6), 11 enriched terms were found for UW1 (Fig. 4d; Supplementary Table 7). From these 11 GOs, six from the Cellular Component (CC) category were under-represented (GO:0005622, “intracellular anatomical structure “; GO:0005634 “nucleus”; GO:0043226, “organelle”; GO:0043227, “membrane-bounded organelle”; GO:0043229, "intracellular organelle”; GO:0043231, “intracellular membrane-bounded organelle”), together with one GO from the Molecular Function (MF) category (GO:0003723, “RNA binding”). On the other hand, over-represented GOs included three terms from the MF category (GO:0003824, “catalytic activity”; GO:0016491, “oxidoreductase activity”; GO:0016740, “transferase activity”) and one from the Biological Process (BP) category (GO:0019748, “secondary metabolic process”).

Table 2 Selected DEGs (LFC > |2|) from the individual response analysis and classified per category. The list is classified based on increasing LFC per category. Negative LFC means down-regulation and positive LFC, up-regulation

Gene ID	Description	LFC	adjusted *P* value
Immune response			
FAR3			
gene41134	peroxidase 42-like [Olea europaea var. sylvestris]	2.07	0.043890762
gene10295	thaumatin-like protein [Olea europaea var. sylvestris]	2.10	0.005621391
gene35979	basic endochitinase-like [Olea europaea var. sylvestris]	2.60	0.028011333
gene16958	peroxidase 12-like [Olea europaea var. sylvestris]	3.08	0.001018325
gene55223	thaumatin-like protein [Olea europaea var. sylvestris]	3.25	0.007501784
gene35829	basic endochitinase-like [Olea europaea var. sylvestris]	3.56	0.006722346
UW1			
gene19486	probable E3 ubiquitin-protein ligase RHA4A [Olea europaea var. sylvestris]	−2.16	0.000528699
gene42370	probable LRR receptor-like serine/threonine-protein kinase At1g53440 [Olea europaea var. sylvestris]	2.27	0.040923708
gene45192	E3 ubiquitin-protein ligase WAV3-like isoform X1 [Salvia splendens]	2.53	0.000516016
gene24831	E3 ubiquitin-protein ligase PUB23-like [Olea europaea var. sylvestris]	2.60	0.000226903
gene39449	E3 ubiquitin-protein ligase RHA2A-like [Olea europaea var. sylvestris]	2.64	9.68284E-06
gene13983	E3 ubiquitin-protein ligase PUB23-like [Olea europaea var. sylvestris]	2.81	1.19797E-05
gene4656	thaumatin-like protein 1b [Olea europaea var. sylvestris]	3.00	0.001886435
gene21955	disease resistance response protein 206-like [Olea europaea var. sylvestris]	3.13	0.001271404
gene50396	thaumatin-like protein [Olea europaea var. sylvestris]	4.47	0.00049578
gene40032	E3 ubiquitin-protein ligase RHA2B-like [Olea europaea var. sylvestris]	4.80	0.010060147
gene4044	E3 ubiquitin-protein ligase RHA2B-like [Olea europaea var. sylvestris]	6.10	0.001713104
Biosynthesis of phenylpropanoids			
FAR3			
gene27831	alpha-glucosidase 2-like isoform X1 [Salvia hispanica]	−2.25	0.038617805
gene51842	glucan endo-1,3-beta-glucosidase 11-like [Olea europaea var. sylvestris]	2.02	0.031951988
gene49788	caffeic acid 3-O-methyltransferase-like isoform X1 [Olea europaea var. sylvestris]	2.31	0.003413624
gene11936	glucan endo-1,3-beta-glucosidase, acidic-like [Olea europaea var. sylvestris]	2.40	8.06383E-09
gene57748	cationic peroxidase 1-like isoform X1 [Olea europaea var. sylvestris]	2.44	1.28637E-05
gene56752	glucan endo-1,3-beta-glucosidase, acidic-like [Olea europaea var. sylvestris]	2.89	3.59041E-09
gene49784	caffeic acid 3-O-methyltransferase-like isoform X1 [Olea europaea var. sylvestris]	3.01	0.027452279
gene41383	glucan endo-1,3-beta-glucosidase, acidic-like [Olea europaea var. sylvestris]	4.09	8.06383E-09
gene44168	beta-glucosidase-like isoform X2 [Olea europaea var. sylvestris]	5.18	0.006463636
UW1			
gene20843	caffeic acid 3-O-methyltransferase-like isoform X1 [Olea europaea var. sylvestris]	−2.69	0.023729714
gene16388	anthocyanidin 3-O-glucoside 2'''-O-xylosyltransferase-like [Olea europaea var. sylvestris]	2.04	0.019145355
gene43130	4-coumarate–CoA ligase 2-like [Olea europaea var. sylvestris]	2.28	0.003825206
gene46772	phenylalanine ammonia-lyase-like isoform X1 [Olea europaea var. sylvestris]	2.39	0.025302066
gene55647	phenylalanine ammonia-lyase-like isoform X1 [Olea europaea var. sylvestris]	2.41	0.032549987
gene49783	caffeic acid 3-O-methyltransferase-like isoform X1 [Olea europaea var. sylvestris]	2.66	0.034830271
gene41383	glucan endo-1,3-beta-glucosidase, acidic-like [Olea europaea var. sylvestris]	3.15	0.001423023
gene1044	beta-glucosidase-like isoform X2 [Olea europaea var. sylvestris]	3.79	0.01085737
gene16778	lignin-forming anionic peroxidase-like [Olea europaea var. sylvestris]	6.86	0.006838628
MVA pathway			
UW1			
gene13507	3-hydroxy-3-methylglutaryl-coenzyme A reductase 1-like [Olea europaea var. sylvestris]	4.18	0.000503877
Transcription factors (TFs)			
FAR3			
gene12571	probable WRKY transcription factor 50 [Olea europaea var. sylvestris]	2.63	0.014620399
gene24961	probable WRKY transcription factor 43 [Olea europaea var. sylvestris]	3.46	0.017570707

Table 2 (continued)

Gene ID	Description	LFC	adjusted *P* value
gene46078	ethylene-responsive transcription factor 1B-like [Olea europaea var. sylvestris]	3.55	0.044879943
gene23853	probable WRKY transcription factor 75 [Olea europaea var. sylvestris]	4.60	0.000561876
gene14628	probable WRKY transcription factor 75 [Olea europaea var. sylvestris]	4.84	0.015247718
UW1			
gene44089	zinc finger protein CONSTANS-LIKE 1-like [Olea europaea var. sylvestris]	−3.14	0.004062066
gene53663	transcription factor HBI1-like isoform X1 [Olea europaea var. sylvestris]	−2.80	0.004181453
gene43402	zinc transporter 1-like [Olea europaea var. sylvestris]	−2.53	3.78953E-08
gene6760	ethylene-responsive transcription factor RAP2-3-like [Olea europaea var. sylvestris]	2.01	0.000363731
gene8650	zinc finger protein ZAT11-like [Olea europaea var. sylvestris]	2.16	0.047851691
gene41945	zinc finger protein ZAT10-like [Olea europaea var. sylvestris]	2.20	0.013287144
gene52243	transcription factor bHLH149-like [Olea europaea var. sylvestris]	2.29	0.001423023
gene33741	transcription factor MYB108-like [Olea europaea var. sylvestris]	2.31	0.00073802
gene8649	zinc finger protein ZAT12-like [Olea europaea var. sylvestris]	2.32	0.046620757
gene27665	zinc finger CCCH domain-containing protein 15-like [Coffea arabica]	2.50	0.006228774
gene24497	transcription factor MYB87-like [Olea europaea var. sylvestris]	2.54	0.021966165
gene7310	transcription factor bHLH78-like isoform X1 [Olea europaea var. sylvestris]	2.59	0.02753492
gene53219	homeobox-leucine zipper protein ATHB-52-like [Andrographis paniculata]	2.83	0.032532312
gene17325	ethylene-responsive transcription factor 1B-like [Olea europaea var. sylvestris]	2.87	2.01471E-05
gene27964	ethylene-responsive transcription factor 1A-like [Olea europaea var. sylvestris]	3.00	0.043138797
gene15014	probable WRKY transcription factor 75 [Olea europaea var. sylvestris]	3.01	0.033389049
gene12571	probable WRKY transcription factor 50 [Olea europaea var. sylvestris]	3.01	0.008329368
gene21136	NAC transcription factor 32-like [Olea europaea var. sylvestris]	3.17	1.70503E-10
gene21335	transcription factor MYB108-like [Olea europaea var. sylvestris]	3.24	0.006654049
gene19400	transcription factor MYB108-like [Olea europaea var. sylvestris]	3.30	0.008020111
gene45787	ethylene-responsive transcription factor ABR1-like [Olea europaea var. sylvestris]	3.32	0.014179135
gene39851	transcription factor MYB114-like [Olea europaea var. sylvestris]	3.40	0.006499166
gene813	probable WRKY transcription factor 75 [Olea europaea var. sylvestris]	3.41	0.007025816
gene45311	NAC domain-containing protein 79-like [Olea europaea var. sylvestris]	3.54	9.0762E-05
gene44635	probable WRKY transcription factor 40 [Olea europaea var. sylvestris]	3.78	7.65368E-10
gene51097	ethylene-responsive transcription factor 1B-like [Olea europaea var. sylvestris]	3.79	0.00177755
gene23287	homeobox-leucine zipper protein HOX11-like isoform X2 [Olea europaea var. sylvestris]	3.81	0.020894037
gene1711	ethylene-responsive transcription factor 1B-like [Olea europaea var. sylvestris]	4.06	0.004062066
gene46078	ethylene-responsive transcription factor 1B-like [Olea europaea var. sylvestris]	4.34	0.047109291
gene6009	transcription factor bHLH93-like [Olea europaea var. sylvestris]	4.36	1.96561E-05
gene56031	zinc finger protein GIS3-like [Olea europaea var. sylvestris]	4.39	0.000224679
gene2954	ethylene-responsive transcription factor 1B-like [Olea europaea var. sylvestris]	4.46	0.00985783
gene25015	ethylene-responsive transcription factor ABR1-like [Olea europaea var. sylvestris]	4.90	0.000194924
gene25842	probable WRKY transcription factor 75 [Olea europaea var. sylvestris]	4.98	2.19796E-05
gene48533	NAC domain-containing protein 2-like [Olea europaea var. sylvestris]	5.28	3.36893E-06
gene27363	transcription factor bHLH162-like [Olea europaea var. sylvestris]	5.34	0.026761909
gene23853	probable WRKY transcription factor 75 [Olea europaea var. sylvestris]	5.54	5.08046E-06
gene56601	transcription factor MYB8-like [Olea europaea var. sylvestris]	5.96	0.021710579
gene25119	ethylene-responsive transcription factor ERF110-like [Olea europaea var. sylvestris]	6.06	0.016848626
gene14628	probable WRKY transcription factor 75 [Olea europaea var. sylvestris]	6.40	0.001125969
Jasmonic acid pathway			
UW1			
gene37552	putative 12-oxophytodienoate reductase 11 [Sesamum indicum]	2.54	0.008228671
Salicylic acid pathway			
FAR3			
gene33656	salicylic acid-binding protein 2-like [Olea europaea var. sylvestris]	2.01	0.014346101

Table 2 (continued)

Gene ID	Description	LFC	adjusted *P* value
gene6437	protein DMR6-LIKE OXYGENASE 2-like [Olea europaea var. sylvestris]	4.27	0.020499253
UW1			
gene33633	salicylic acid-binding protein 2-like [Olea europaea var. sylvestris]	2.63	0.001371967
Ethylene pathway			
UW1			
gene43829	1-aminocyclopropane-1-carboxylate oxidase-like [Olea europaea var. sylvestris]	2.80	0.00011535
gene53843	1-aminocyclopropane-1-carboxylate synthase-like [Olea europaea var. sylvestris]	3.26	2.63325E-05
gene12137	1-aminocyclopropane-1-carboxylate synthase-like [Olea europaea var. sylvestris]	3.54	1.24589E-05
gene43841	1-aminocyclopropane-1-carboxylate oxidase-like [Olea europaea var. sylvestris]	3.57	3.42964E-14
gene28206	1-aminocyclopropane-1-carboxylate synthase-like [Olea europaea var. sylvestris]	4.06	4.60667E-05
gene11437	1-aminocyclopropane-1-carboxylate oxidase 1-like [Olea europaea var. sylvestris]	4.29	0.000104275
gene2877	1-aminocyclopropane-1-carboxylate oxidase homolog 1-like [Olea europaea var. sylvestris]	4.30	5.92876E-09

DEGs commonly regulated by both genotypes

After considering the individual modulations that took place in each genotype, we then repeated the differential gene expression analysis including both genotype and treatment as variables (see Methods). A total of 512 significant DEGs were identified and are listed in Supplementary Table 8. To further explore this list, we performed a hierarchical clustering using z-scores transformation per transcript, and four main clusters could be identified (Fig. 5a). Although there was a slight difference in the level of the response between biological replicates within clusters, common patterns of up- or down-regulation were sufficiently conserved between the treatments. There were a higher number of strongly up-regulated genes in the infected groups, as seen in clusters 1 and 3 for both genotypes (Fig. 5a).

We were then interested in comparing the three lists of DEGs generated from the common versus the individual response approaches. The nine genes presented in the individual analysis were also identified in the common analysis (Fig. 5b). 220 DEGs corresponding to 23% of the total were exclusively identified in the common response analysis, while 69 for FAR3 and 214 for UW1 were also found in the individual response approach (Fig. 5b; Supplementary Table 9). In total, as shown in the Venn diagram, 152 DEGs (15.9%) for FAR3 and 292 (30.5%) for UW1 were only identified in the individual analysis.

Next, we screened the resulting common response list for strongly modulated DEGs (LFC > |2|) using the same keyword-set used to categorize DEGs in the individual response (Supplementary Table 8). Among the DEGs that differed from the individual analysis, eight leucine-rich repeat (LRR) proteins were found (gene1307, gene13877, gene15810, gene27011, gene30540, gene41689, gene44119, and gene49570), either up- or down-regulated in both genotypes (Table 3). Additionally, gene6437 and gene6456 were annotated as protein DMR6-LIKE OXYGENASE 2-like and were strongly up-regulated in FAR3 and UW1, and several components of the phenylpropanoid pathway were significantly modulated (Table 3).

Lastly, we performed a two-tailed SEA of DEGs from the common response (Supplementary Table 8) resulting in eight enriched GO terms (Fig. 5c; Supplementary Table 10). Over-represented terms belonged to the BP (GO:0009719, "response to endogenous stimulus"; GO:0042221, "response to chemical"; GO:0050896, "response to stimulus") and MF (GO:0003824, "catalytic activity") categories, while terms from the CC category were found to be under-represented (GO:0043226, "organelle"; GO:0043227, "membrane-bounded organelle"; GO:0043229, "intracellular organelle"; GO:0043231, "intracellular membrane-bounded organelle").

Discussion

Among research efforts to halt ash dieback spread, understanding the genetic diversity of the host underlying heritable susceptibility is of key importance for future breeding and management initiatives (Pautasso et al. 2013). In the present study, we selected two ash genotypes with lower (FAR3) and higher (UW1) susceptibility to ADB originated from natural German ash populations. Our study showed that the more susceptible genotype UW1 showed more than twice as many DEGs (515) in the individual response as the less susceptible FAR3 (230). Among UW1 DEGs, several transcripts involved in cell wall metabolism and lignification were modulated (e.g., laccase-1-like, laccase-15-like; laccase-14-like; cinnamoyl-CoA reductase 1-like; cellulose synthase-like protein E6, among others, Supplementary Table 4), including the overrepresentation of the GO term secondary metabolic process. In conifers, lignification increases during fungal infection to prevent hyphal

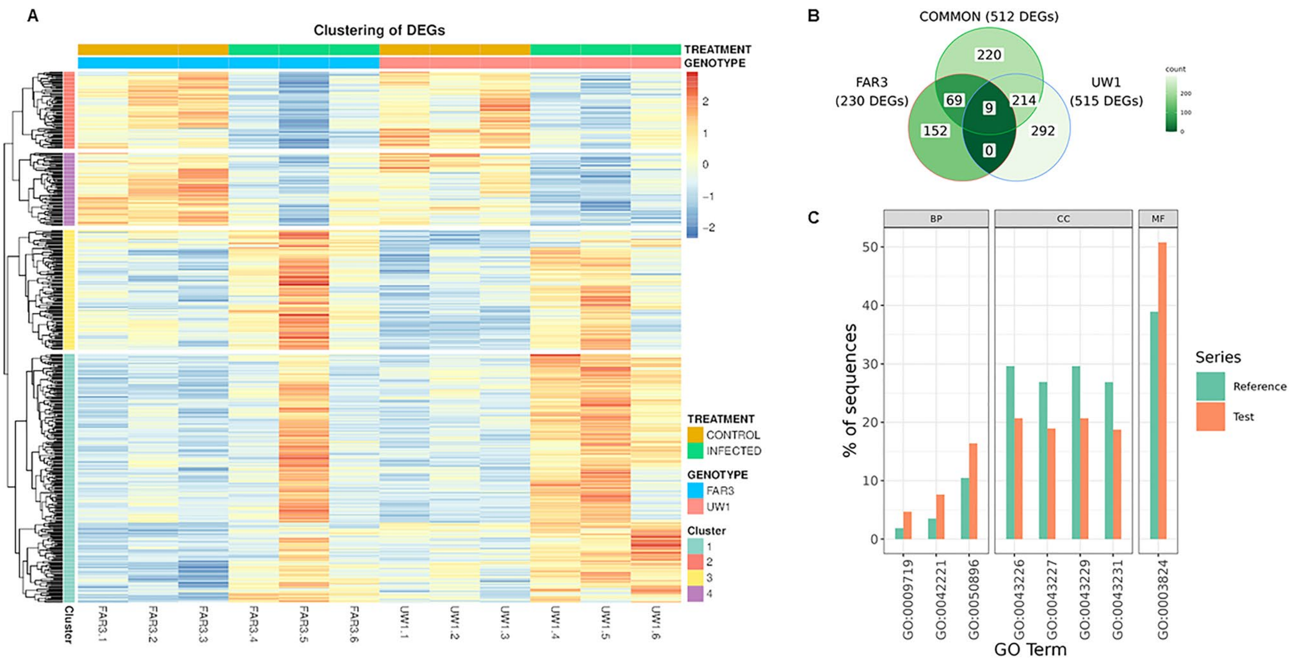

Fig. 5 Analysis of the common response between European ash genotypes and comparison to each genotype individually. Leaf rachises from ash trees with higher (UW1) and lower (FAR3) susceptibility to ash dieback were sampled after seven days of inoculation with infected and uninfected wooden plugs. The analysis for the common responses used both genotypes and treatments as variables for the differential expression analysis, whereas the individual response compared treatments for each genotype separately. **A** Hierarchical clustering of differentially expressed genes (DEGs). Color scale from blue to orange indicates z-scores of transformed (vst) values per transcript. Groupings for genotype, treatment and cluster numbers are shown. **B** Venn diagram of DEGs comparing the analysis for the common and individual responses. Values show DEGs up- or down-regulated at adjusted *P* value <0.05 and $\log_2$ fold change (FC) $>|1|$. Color scale indicates the number of DEGs. The same nine DEGs shown in Fig. 3 are also at the intersection here. **C** Enriched GO terms identified using simple enrichment analysis (SEA) using the list of DEGs for the common response. Over-represented GOs are those with a higher percentage of sequences in the test (list of DEGs) than in the reference (complete list of gene models), while the percentage of sequences in under-represented GOs is higher in the reference set. The description for the highlighted GO terms is as follows: GO:0009719 response to endogenous stimulus; GO:0042221 response to chemical; GO:0050896 response to stimulus; GO:0043226 organelle; GO:0043227 membrane-bounded organelle; GO:0043229 intracellular organelle; GO:0043231 intracellular membrane-bounded organelle; GO:0003824 catalytic activity *BP* biological process; *CC* cellular component; *MF* molecular function; *GO* Gene Ontology

penetration, especially in *Pinus* species resistant to *Fusarium circinatum*, and a role for phenylalanine ammonia-lyase (PAL) in linking primary and secondary metabolism has been reported (Zamora-Ballesteros et al. 2021). Here, however, we observed an opposite pattern, with lignification-related transcripts being most prominent in the susceptible ash genotype. This could also be a response to the trophic behavior of the pathogen, as *F. circinatum* is a necrotrophic species (Morse et al. 2004) and forces the host to actively lignify the infected area, while *H. fraxineus* follows an initially biotrophic strategy (Mansfield et al. 2019). Since *H. fraxineus* presents both a necrotrophic and biotrophic phase of infection, clearly there is a complex nature of the host genotype-dependent response in *F. excelsior* (Gross et al. 2014).

In addition, our analysis revealed significantly up-regulated transcripts for the 3-hydroxy-3-methylglutaryl-coenzyme A reductase 1-like (LFC = 4.18, adjusted *P* value 0.0005) in UW1 (Table 2). This transcript encodes an enzyme that catalyzes the synthesis of mevalonate in the isoprenoid pathway in plants (Learned and Fink 1989). As an important marker, it has been reported that the production of iridoid glycosides, which are terpenoid-derivatives, was lower in less susceptible ash trees (Sambles et al. 2017; Sollars et al. 2017). Iridoid glycosides are involved in anti-herbivory functions and, hence, were reported to be present in higher concentrations in *F. excelsior* leaves under the attack of emerald ash borer (Chen et al. 2011; Qazi et al. 2018). This may mean, however, that breeding for lower iridoid glycosides may increase the susceptibility to other biotic agents (Sambles et al. 2017).

In terms of secondary metabolism, phenylpropanoids are an essential part of the defense metabolism (Zaynab et al. 2018). Here, we observed that both genotypes showed up-regulation of several DEGs involved in phenylpropanoid biosynthesis, differing in the fact that FAR3, the less

Table 3 Selected DEGs from the common response analysis and classified per category. Only results that differed from the individual response analysis are shown. Negative LFC values indicates down-regulation and positive LFC, up-regulation. The complete list is available in Supplementary Table 7

Gene ID	Description	adjusted *P* value	LFC, FAR3	LFC, UW1
Immune response				
gene1307	leucine-rich repeat extensin-like protein 6 [Olea europaea var. sylvestris]	0.0020062	−1.62	−1.95
gene13877	probable LRR receptor-like serine/threonine-protein kinase At1g56140 isoform X1 [Olea europaea var. sylvestris]	0.0170021	−1.50	−1.42
gene15810	probable LRR receptor-like serine/threonine-protein kinase At5g63710 isoform X1 [Olea europaea var. sylvestris]	0.029179	−1.35	−1.11
gene27011	probable LRR receptor-like serine/threonine-protein kinase At5g63710 isoform X2 [Olea europaea var. sylvestris]	0.0270392	1.00	1.41
gene30540	LRR receptor-like serine/threonine-protein kinase EFR [Olea europaea var. sylvestris]	0.0479516	1.21	0.99
gene41689	leucine-rich repeat extensin-like protein 3 [Olea europaea var. sylvestris]	0.049509	1.67	3.17
gene44119	probable LRR receptor-like serine/threonine-protein kinase At2g23950 [Olea europaea var. sylvestris]	0.0301822	1.83	0.59
gene49570	LRR receptor-like serine/threonine-protein kinase [Olea europaea var. sylvestris]	0.0234073	2.35	3.06
gene4656	thaumatin-like protein 1b [Olea europaea var. sylvestris]	0.0314467	2.08	3.20
gene55223	thaumatin-like protein [Olea europaea var. sylvestris]	0.0363116	3.06	0.73
Salicylic acid pathway				
gene6437	protein DMR6-LIKE OXYGENASE 2-like [Olea europaea var. sylvestris]	0.0173918	3.90	3.70
gene6456	protein DMR6-LIKE OXYGENASE 2-like [Olea europaea var. sylvestris]	0.0301204	3.93	3.45
Biosynthesis of phenylpropanoids				
gene43130	4-coumarate–CoA ligase 2-like [Olea europaea var. sylvestris]	0.0161129	1.78	1.74
gene1044	beta-glucosidase-like isoform X2 [Olea europaea var. sylvestris]	0.0343985	−2.38	−2.44
gene11936	glucan endo-1,3-beta-glucosidase, acidic-like [Olea europaea var. sylvestris]	0.0156	−1.71	−1.75
gene41383	glucan endo-1,3-beta-glucosidase, acidic-like [Olea europaea var. sylvestris]	0.0226535	1.64	4.27
gene49782	caffeic acid 3-O-methyltransferase-like isoform X1 [Olea europaea var. sylvestris]	0.0436593	2.42	4.30
gene49783	caffeic acid 3-O-methyltransferase-like isoform X1 [Olea europaea var. sylvestris]	0.0253309	2.42	3.06
gene49787	caffeic acid 3-O-methyltransferase-like isoform X1 [Olea europaea var. sylvestris]	0.0453388	2.42	2.37
gene49788	caffeic acid 3-O-methyltransferase-like isoform X1 [Olea europaea var. sylvestris]	0.0051741	2.42	0.81
gene56752	glucan endo-1,3-beta-glucosidase, acidic-like [Olea europaea var. sylvestris]	1.9E-06	3.40	4.38

susceptible genotype, presented up-regulation of a peroxidase 42-like and down-regulation of an alpha-glucosidase 2-like isoform X1, whereas UW1 showed down-regulation of caffeic acid 3-O-methyltransferase-like isoform X1. Several genes involved in the phenylpropanoid pathway were also significantly differentially expressed in the common response analysis, further confirming the modulation in both genotypes. A similar response including specific peroxidase modulations, has been reported in both resistant and susceptible genotypes of American elm infected with *Ophiostoma novo-ulmi* (Islam et al. 2022). Thus, phenylpropanoid metabolism alone does not appear to be able to distinguish between trees with different susceptibility to ADB.

Plants have evolved a complex immune system based on two levels. The first is the pattern-triggered immunity (PTI) and is activated upon recognition of pathogen elicitors, such as pathogen- or microbial-associated molecular patterns (PAMPs/MAMPs) by transmembrane pattern recognition receptors (PRRs). However, pathogens have also developed molecular mechanisms to block PTI by using effectors, inducing the so-called effector-triggered susceptibility (ETS). Therefore, the second level of plant immunity involves the expression of R (resistance) genes after ETS, encoding proteins such as nucleotide-binding leucine-rich repeats (NB-LRRs) (Jones and Dangl 2006). NB-LRRs recognize pathogen effectors and induce the effector-triggered immunity (ETI), which in turn activates downstream cascades and enhances PTI (Yuan et al. 2021). In the common response analysis performed here, several LRR proteins were up- and down-regulated (Table 3), suggesting the activation of ETI and subsequent potentiation of PTI in both genotypes. The PTI + ETI response activates phytohormone biosynthesis. Responses mediated by JA and ET are more common in cases of necrotrophic pathogens, whereas the SA–dependent pathway is mostly activated in biotrophic infections (Glazebrook 2005; Huang et al. 2020). It has also been shown that there is a temporal balance with blurred boundaries between JA, ET, and SA-mediated responses, especially when attacked by hemibiotrophic fungi (Ding et al. 2011).

FAR3, the less susceptible genotype, showed concomitant up-regulation of salicylic acid-binding protein 2-like (LFC = 2.01) and protein DMR6-like oxygenase 2-like (LFC = 4.27). DMR6-like oxygenase has been reported to suppress the immune response by repressing the SA pathway, which has been previously connected to susceptibility to mildew infections (Zeilmaker et al. 2015). Although DMR6-like oxygenase was also up-regulated in the common response analysis, we considered it more relevant in the context of FAR3 alone, since other hormone-related pathways were not induced at similar levels in this genotype. This may indicate a more stringent control in FAR3 of the hypersensitive response (HR), which is triggered by SA, and the subsequent programmed cell death (PCD) in the pathogen-infected area, promoting necrosis and limiting further spread of the infection by nutrient deprivation, but also negatively affecting host tissues (Balint-Kurti 2019). Indeed, the higher peroxidase activity and expression of reductases in FAR3 might also be related to detoxification processes and scavenging of reactive oxygen species (ROS), involved in the initiation of the HR. Finally, the most up-regulated TFs in FAR3 belonged to the WRKY family, which are reported to be involved in immune responses and to mediate SA and JA responses (Glazebrook 2005; Eulgem and Somssich 2007). In particular, WRKY75 regulates JA responses against necrotrophic pathogens (Chen et al. 2021). Although different homologs of WRKY75 were present in both genotypes, higher LFC values were found in the less susceptible genotype FAR3. Overall, it seems that a JA-mediated response may control the switch from biotrophic to necrotrophic behavior of *H. fraxineus*, while a SA-mediated response, inducing the production of PR-proteins and subsequently phenylpropanoids, is also activated in the early stages of ADB. A similar response has been observed in the case of Dutch elm disease, which affects the European field elm (*Ulmus minor* Mill.) (Chano et al. in prep.).

In our study, FAR3 showed six up-regulated transcripts (LFC > 2) classified as part of the immune system, annotated as thaumatin-like proteins (gene55223 and gene55223), peroxidases-like proteins (gene41134 and gene16958), and basic endochitinase-like proteins (gene35979 and gene35829) (Table 2), which classify as pathogen-related (PR) proteins. Thaumatin-like proteins and peroxidases are assigned to PR-5 and PR-9 and show reportedly antifungal roles (Jain and Khurana 2018). Chitinases are actually PR-like proteins (PRLs), usually involved in fungal cell wall degradation, and have been induced by SA-mediated responses in pine seedlings challenged by the necrotrophic *Fusarium subglutinans* f. sp. *pini* (Davis et al. 2002).

In contrast to this concise and restrained response, several DEGs annotated as E3 ubiquitin-protein ligases (i.e., types RHA4A, RHA2B, WAV-3, PUB23) were up-regulated in UW1, leading to the overrepresentation of the GO terms catalytic and transferase activity. Ubiquitination is a post-translational modification that feedbacks and controls plant immune responses, since, when in excess, immune responses may be detrimental to plant growth and promote autoimmunity by unbalanced HR and PCD (You et al. 2016; Chen et al. 2022). Interestingly, GO terms for endomembrane trafficking were under-represented in UW1 (Supplementary Figure S1), supported by up-regulation (LFC = 2.6) of the E3 ubiquitin-protein ligase PUB23-like, which is reported to attenuate chitin-elicited responses by controlling endomembrane trafficking of plant immune receptors, thereby reducing PAMP-triggered responses (Stegmann et al. 2012; Chen et al. 2022). Transcripts for PR-5 (thaumatin-like proteins) and a disease resistance response protein 206-like were up-regulated in UW1, the latter also reported to support the resistance of melon (*Cucumis melo*) to Fusarium wilt disease (Yang et al. 2022). Among the TFs strongly up-regulated in UW1, the bHLH family has been reported to be involved in iridoid metabolism in *Catharanthus roseus* (Van Moerkercke et al. 2015). As well, up-regulated transcripts for numerous ET-responsive TFs and 1-aminocyclopropane-1-carboxylate oxidase-like/synthase-like suggested an ET-mediated immune response, which would be expected for necrotrophic pathogens such as *H. fraxineus*. Therefore, one possible interpretation is that, in the more susceptible genotype UW1, the elicited response is fast and strong, triggering a self-controlled mechanism that may ultimately limit the effectiveness of the defense against the infection, and contribute to increased susceptibility.

The current work focused on the transcriptional changes in *F. excelsior* trees that occur in the leaf rachis 7 days after ADB infection, representing, to the best of our knowledge, one of the earliest samplings for RNA-seq performed in ash after infection. We used the inoculation procedure described by Schwanda and Kirisits (2016), but they evaluated the first symptoms after 20 days. When using a transcriptomic approach to study molecular host responses to pathogen infections, it is critical to focus on the initial steps of the disease (Arce-Leal et al. 2020). Although molecular changes can occur within seconds, here we considered seven days as an early stage of the infection since the disease develops and shows symptoms over the course of months in nature (Gross and Holdenrieder 2013). In the present study, seven days allowed for the detection of significant transcriptional changes when comparing control and infected groups of samples. At the same time, no GO enriched terms were found for one of the genotypes, and these results combined may reinforce that transcriptional changes associated with ash dieback in ash trees take place slowly, as also suggested for tanoak (Hayden et al. 2014), further indicating that seven days post-infection is probably the minimum period to start monitoring expressional changes in response to ADB. Mansfield et al. (2018) performed ascospore inoculations on *F. excelsior* leaves and reported the first visible symptoms already after seven days.

Although different pathosystems are very species-dependent, similar monitoring times have been chosen in other tree species, such as in tanoak infected with *Phytophthora ramorum* (Hayden et al. 2014) and *Pinus pinaster* under *Fusarium circinatum* challenge (Hernandez-Escribano et al. 2020). Samplings during shorter incubation times have also been performed, as in samples taken only 96 h after inoculation with *Ophiostoma novo-ulmi* on American elms (Islam et al. 2022), and after only one and two hours post-inoculation with *Erwinia amylovora* on apple (*Malus* x *domestica*) (Norelli et al. 2009). These studies, like the present one, indicate it is possible to evaluate the early stages of the infection with useful outcomes.

Furthermore, we observed that the general trends in transcriptional modulation were consistent within each genotype (Fig. 5a), with some individual variation between our replicates (Fig. 3). This could be explained by temporal differences in the success of the infection process, reinforced by the absence of symptoms in some of the replicates (data not shown), resulting in a heterogeneous time frame of response between individual trees. Another source of variation may be a small but different amount of pathogen material, which may have grown differently on the wooden sticks used for inoculation. We highlight this as a potential limitation of working with wooden sticks as inoculants. In addition, we worked with grafted replicates of the same genotype with individual rootstocks. Ideally, plants derived from in vitro culture or rooted cuttings should be used to avoid rootstock effects.

Finally, the monitoring of the exact time point after infection is a challenging feature in natural populations, highlighting the value of studies under controlled conditions to characterize the molecular mechanisms of host and pathogen responses in a timely manner. However, set-ups have differed in the literature in terms of type of inoculation, tissue, and duration of the experiments, leaving room for multiple strategies that may influence the results. Here, we artificially inoculated leaf rachises with wood plugs and found a detectable transcriptional response seven days later, even though signs of necrosis were not visible at that time. In previous attempts to assess ADB susceptibility, ash wood plugs were used for bark inoculations at breast height and the disease spread was monitored for two years (Lobo et al. 2015). In another experiment testing for a phylogenetic signal in disease susceptibility, leaf and stem inoculations with ash wood plugs were monitored for 6–18 months in European, Asian and North American ash species (Nielsen et al. 2017). Moreover, by selecting uninfected ash branches and performing bark inoculations with infested agar plugs, a transcriptional profiling of the tissue was performed after 10 months (Sahraei et al. 2020). In another study, ash petioles were sampled following rachis inoculation with ash wood plugs after three months to compare variance in disease susceptibility using quantitative polymerase chain reaction (qPCR) assays (Nielsen et al. 2022). In fact, the typical and natural way of infection for ADB is through ascospores landing on the leaf surface, but no transcriptional study has focused on this aspect so far. In particular, a focus on the typical pathway of infection over the leaf surface might reveal insights into early response mechanisms. However, ascospore solutions as inoculants are challenging, because ascospores are only viable for a short time window, which may reduce inoculation efficacy (Schlegel et al. 2016; Mansfield et al. 2018).

In summary, the aim of the current study was to provide initial insights into the early transcriptional component of susceptibility to ADB. It is clear that future experiments including a higher number of genotypes with distinct levels of susceptibility and sampling at different time points after inoculation will contribute to a wider and deeper understanding of the molecular mechanisms in response to ADB. Following more robust experiments to confirm and possibly select new DEGs involved in heritable susceptibility to ADB using transcriptomics, further verification in independent experiments using additional genotypes and methods to target specifically these DEGs, such as qPCR will be necessary.

Conclusions

We investigated the transcriptional changes in two ash genotypes from Germany with different susceptibility levels. Our work with mock-inoculated and pathogen-inoculated ash trees indicated that significant changes at the transcriptional level could be detected seven days after the start of the experiment. This work allowed for a comparison of analytical approaches, in terms of differential expression analysis, including both variables (genotypes + treatments), or control versus infected groups for each genotype. Overall, transcriptomics provided a valid approach to hint toward a stronger but possibly less targeted metabolic response in the more susceptible genotype (UW1), which may be more JA- and ET-mediated but may have caused a feedback loop that hindered the plant immune response. In contrast, the less susceptible genotype appeared to respond in a more targeted manner, mediated exclusively by the SA pathway, which might be more efficient and thus contribute to reduced susceptibility.

Availability of data and code

The sequencing data from the twelve samples used in this work have been deposited in the NCBI Sequence Read Archive (SRA) under the BioProject accession no.

PRJNA1024896, SRA accession no. from SRR26302913 to SRR26302924 (http://www.ncbi.nlm.nih.gov/sra/). The code and scripts used for this article can be found at https://github.com/vchano/fraxgen_assay.

Supplementary Information The online version contains supplementary material available at https://doi.org/10.1007/s41348-024-01028-3.

Acknowledgements We would like to thank Dr. Wilfried Steiner, Martin Dreist, Hartmut Frege and Thilo Schuppelius for grafting the trees and Alexandra Dolynska, Gudrun Diederich, Gerold Dinkel and Daniel Teklemariam for their support during greenhouse work. We also thank Dr. Bartosz Ulaszewski and Dr. Joanna Meger for sharing the new reference genome and gene model with us prior to publication. The FraxGen subproject (2219WK21F4) was part of the FraxForFuture consortium, funded by the Waldklimafonds (WKF) which itself is funded by the German Federal Ministry of Food and Agriculture (BMEL) and the Federal Ministry for the Environment, Nature Conservation, Nuclear Safety and Consumer Protection (BMUV) administrated by the Agency for Renewable Resources (FNR). This work used the Scientific Compute Cluster at GWDG, the joint data center of Max Planck Society for the Advancement of Science (MPG) and University of Göttingen.

Author contributions OG and KBB contributed to conceptualization; OG contributed to funding acquisition; RCF, VC, KBB, TDF and KS contributed to methodology and investigation; RCF and VC carried out analysis; RCF performed original draft preparation; all performed writing—editing and revising; KBB and OG carried out project administration.

Funding Open Access funding enabled and organized by Projekt DEAL. Waldklimafonds, 2219WK21F4, Oliver Gailing

Declarations

Conflict of interest The authors declare no conflict of interest.

References

Al-Shahrour F, Díaz-Uriarte R, Dopazo J (2004) FatiGO: a web tool for finding significant associations of gene ontology terms with groups of genes. Bioinform 20(4):578–580. https://doi.org/10.1093/bioinformatics/btg455

Anders S, Pyl PT, Huber W (2015) HTSeq—a python framework to work with high-throughput sequencing data. Bioinform 31(2):166–169. https://doi.org/10.1093/bioinformatics/btu638

Arce-Leal ÁP, Bautista R, Rodríguez-Negrete EA et al (2020) Gene expression profile of Mexican Lime (*Citrus aurantifolia*) trees in response to Huanglongbing disease caused by *Candidatus liberibacter asiaticus*. Microorganisms 8:528. https://doi.org/10.3390/microorganisms8040528

Balint-Kurti P (2019) The plant hypersensitive response: concepts, control and consequences. Mol Plant Pathol 20(8):1163–11178. https://doi.org/10.1111/mpp.12821

Baral H-O, Queloz V, Hosoya T (2014) *Hymenoscyphus fraxineus*, the correct scientific name for the fungus causing ash dieback in Europe. IMA Fungus 5:79–80. https://doi.org/10.5598/imafungus.2014.05.01.09

Bell S, et al (2008) Cultural aspects of the trees in selected European countries. Europe Science Foundation—COST Office. https://bibliotecadigital.ipb.pt/handle/10198/3913?locale=en

Benjamini Y, Hochberg Y (1995) Controlling the false discovery rate: a practical and powerful approach to multiple testing. J R Stat 57:289–300. https://doi.org/10.1111/j.2517-6161.1995.tb02031.x

Blighe K, Rana S, Lewis M (2018) EnhancedVolcano: publication-ready volcano plots with enhanced colouring and labeling. https://github.com/kevinblighe/EnhancedVolcano

Bolger AM, Lohse M, Usadel B (2014) Trimmomatic: a flexible trimmer for illumina sequence data. Bioinform 30(15):2114–2120. https://doi.org/10.1093/bioinformatics/btu170

Budde KB, Nielsen LR, Ravn HP, Kjær ED (2016) The natural evolutionary potential of tree populations to cope with newly introduced pests and pathogens—lessons learned from forest health catastrophes in recent decades. Curr Forestry Rep 2:18–29. https://doi.org/10.1007/s40725-016-0029-9

Camacho C, Coulouris G, Avagyan V, Ma N, Papadopoulos J, Bealer K, Madden TL (2008) BLAST+: architecture and applications. BMC Bioinform 10:421. https://doi.org/10.1186/1471-2105-10-421

Chen Y, Whitehill JGA, Bonello P, Poland TM (2011) Differential response in foliar chemistry of three ash species to emerald ash borer adult feeding. J Chem Ecol 37:29–39. https://doi.org/10.1007/s10886-010-9892-1

Chen L, Zhang L, Xiang S et al (2021) The transcription factor WRKY75 positively regulates jasmonate-mediated plant defense to necrotrophic fungal pathogens. J Exp Bot 72(4):1473–1489

Chen Y, Song Y, Liu J et al (2022) Ubiquitination of receptorsomes, frontline of plant immunity. Int J Mol Sci 23:2937. https://doi.org/10.3390/ijms23062937

Cleary MR, Daniel G, Stenlid J (2013) Light and scanning electron microscopy studies of the early infection stages of *Hymenoscyphus pseudoalbidus* on *Fraxinus excelsior*. Plant Pathol 62:1294–1301. https://doi.org/10.1111/ppa.12048

Davis JM, Wu H, Cooke JEK, Reed JM, Luce KS, Michler CH (2002) Pathogen challenge, salicylic acid, and jasmonic acid regulate expression of chitinase gene homologs in pine. Mol Plant Microbe Interact 15:380–387. https://doi.org/10.1094/MPMI.2002.15.4.380

Ding L, Xu H, Yi H, Yang L, Kong Z, Zhang L, Xue S, Jia H, Ma Z (2011) Resistance to hemi-biotrophic *F. graminearum* infection is associated with coordinated and ordered expression of diverse defense signaling pathways. PLoS ONE 6:e19008. https://doi.org/10.1371/journal.pone.0019008

Enderle R, Stenlid J, Vasaitis R (2019) An overview of ash (*Fraxinus* spp.) and the ash dieback disease in Europe. CABI Rev 2019:1–12. https://doi.org/10.1079/PAVSNNR201914025

Eulgem T, Somssich IE (2007) Networks of WRKY transcription factors in defense signaling. Curr Opin Plant Biol 10:366–371. https://doi.org/10.1016/j.pbi.2007.04.020

Ewels P, Magnusson M, Lundin S, Käller M (2016) MultiQC: summarize analysis results for multiple tools and samples in a single report. Bioinform 32(19):3047–3048. https://doi.org/10.1093/bioinformatics/btw354

Gao CH, Yu G, Cai P (2021) ggVennDiagram: an intuitive, easy-to-use, and highly customizable R package to generate venn diagram. Front Genet 12:1598. https://doi.org/10.3389/fgene.2021.706907

Glazebrook J (2005) Contrasting mechanisms of defense against biotrophic and necrotrophic pathogens. Annu Rev Phytopathol 43:205–227. https://doi.org/10.1146/annurev.phyto.43.040204.135923

Götz S, García-Gómez JM, Terol J, Williams TD, Nagaraj SH, Nueda MJ, Robles M, Talón M, Dopazo J, Conesa A (2008) High-throughput functional annotation and data mining with the Blast2GO suite. Nucleic Acids Res 36:3420–3435. https://doi.org/10.1093/nar/gkn176

Gross A, Holdenrieder O (2013) On the longevity of *Hymenoscyphus pseudoalbidus* in petioles of *Fraxinus excelsior*. For Path 43:168–170. https://doi.org/10.1111/efp.12022

Gross A, Holdenrieder O, Pautasso M et al (2014) *Hymenoscyphus pseudoalbidus*, the causal agent of European ash dieback. Mol Plant Pathol 15:5–21. https://doi.org/10.1111/mpp.12073

Hayden KJ, Garbelotto M, Knaus BJ et al (2014) Dual RNA-Seq of the plant pathogen *Phytophthora ramorum* and its tanoak host. Tree Genet Genomes 10:489–502. https://doi.org/10.1007/s11295-014-0698-0

Hernandez-Escribano L, Visser EA, Iturritxa E, Raposo R, Naidoo S (2020) The transcriptome of *Pinus pinaster* under *Fusarium circinatum* challenge. BMC Genom 21:28. https://doi.org/10.1186/s12864-019-6444-0

Heuertz M, Fineschi S, Anzidei M, Pastorelli R, Salvini D, Paule L, Frascaria-Lacoste N, Hardy OJ, Vekemans X, Vendramin GG (2004a) Chloroplast DNA variation and postglacial recolonization of common ash (*Fraxinus excelsior* L.) in Europe. Mol Ecol 13:3437–3452. https://doi.org/10.1111/j.1365-294X.2004.02333.x

Heuertz M, Hausman J-F, Hardy OJ, Vendramin GG, Frascaria-Lacoste N, Vekemans X (2004b) Nuclear microsatellites reveal contrasting patterns of genetic structure between western and southeastern European populations of the common ash (*Fraxinus excelsior* L.). Evolution 58:976–988. https://doi.org/10.1111/j.0014-3820.2004.tb00432.x

Huang S, Zhang X, Dilantha-Fernando WG (2020) Directing trophic divergence in plant-pathogen interactions: antagonistic phytohormones with NO doubt? Front Plant Sci 11:600063. https://doi.org/10.3389/fpls.2020.600063

Islam MT, Coutin JF, Shukla M et al (2022) Deciphering the genome-wide transcriptomic changes during interactions of resistant and susceptible genotypes of American elm with *Ophiostoma novo-ulmi*. JoF 8:120. https://doi.org/10.3390/jof8020120

Jones JDG, Dangl JL (2006) The plant immune system. Nature 444:323–329. https://doi.org/10.1038/nature05286

Kim D, Paggi JM, Park C, Bennett C, Salzberg SL (2019) Graph-based genome alignment and genotyping with HISAT2 and HISAT-genotype. Nature Biotechnol 37(8):907–915. https://doi.org/10.1038/s41587-019-0201-4

Kolde R (2019) pheatmap: pretty heatmaps. R package version 1.0.12, https://CRAN.R-project.org/package=pheatmap

Kowalski T (2006) *Chalara fraxinea* sp. nov. associated with dieback of ash (*Fraxinus excelsior*) in Poland. For Pathol 6:264–270. https://doi.org/10.1111/j.1439-0329.2006.00453.x

Kräutler K, Kirisits T (2012) The ash dieback pathogen *Hymenoscyphus pseudoalbidus* is associated with leaf symptoms on ash species (*Fraxinus* spp.). J Agric Ext Rural Dev. https://doi.org/10.5897/JAERD12.065

Langer GJ, Fuchs S, Osewold J et al (2022) FraxForFuture—research on European ash dieback in Germany. J Plant Dis Prot 129:1285–1295. https://doi.org/10.1007/s41348-022-00670-z

Learned RM, Fink GR (1989) 3-Hydroxy-3-methylglutaryl-coenzyme A reductase from *Arabidopsis thaliana* is structurally distinct from the yeast and animal enzymes. PNAS 86:2779–2783. https://doi.org/10.1073/pnas.86.8.2779

Li H, Handsaker B, Wysoker A, Fennell T, Ruan J, Homer N, Marth G, Abecasis G, Durbin R (2009) The sequence alignment/map format and SAMtools. Bioinform 25:2078–2079. https://doi.org/10.1093/bioinformatics/btp352

Lobo A, McKinney LV, Hansen JK, Kjær ED, Nielsen LR (2015) Genetic variation in dieback resistance in *Fraxinus excelsior* confirmed by progeny inoculation assay. For Pathol 45:379–387. https://doi.org/10.1111/efp.12179

Love MI, Huber W, Anders S (2014) Moderated estimation of fold change and dispersion for RNA-seq data with DESeq2. Genome Biol 15:550. https://doi.org/10.1186/s13059-014-0550-8

Mansfield JW, Galambos N, Saville R (2018) The use of ascospores of the dieback fungus *Hymenoscyphus fraxineus* for infection assays reveals a significant period of biotrophic interaction in penetrated ash cells. Plant Pathol 67:1354–1361. https://doi.org/10.1111/ppa.12844

Mansfield J, Brown I, Papp-Rupar M (2019) Life at the edge—the cytology and physiology of the biotroph to necrotroph transition in *Hymenoscyphus fraxineus* during lesion formation in ash. Plant Pathol J 68:908–920. https://doi.org/10.1111/ppa.13014

McKinney LV, Nielsen LR, Hansen JK, Kjær ED (2011) Presence of natural genetic resistance in *Fraxinus excelsior* (Oleraceae) to *Chalara fraxinea* (Ascomycota): an emerging infectious disease. Heredity 106:788–797. https://doi.org/10.1038/hdy.2010.119

McKinney LV, Thomsen IM, Kjaer ED, Nielsen LR (2012) Genetic resistance to *Hymenoscyphus pseudoalbidus* limits fungal growth and symptom occurrence in *Fraxinus excelsior*: Genetic resistance to *H. pseudoalbidus*. For Pathol 42:69–74. https://doi.org/10.1111/j.1439-0329.2011.00725.x

Meger J, Ulaszewski B, Pałucka M, Kozioł C, Burczyk J (2024) Genomic prediction of resistance to Hymenoscyphus fraxineus in common ash (*Fraxinus excelsior* L.) populations. Evol Appl 17:e13694. https://doi.org/10.1111/eva.13694

Morse AM, Nelson CD, Covert SF et al (2004) Pine genes regulated by the necrotrophic pathogen *Fusarium circinatum*. Theor Appl Genet 109:922–932. https://doi.org/10.1007/s00122-004-1719-4

Müller M, Kües U, Budde KB, Gailing O (2023) Applying molecular and genetic methods to trees and their fungal communities. Appl Microbiol Biotechnol 107:2783–2830. https://doi.org/10.1007/s00253-023-12480-w

Muñoz F, Marçais B, Dufour J, Dowkiw A (2016) Rising out of the ashes: additive genetic variation for crown and collar resistance to Hymenoscyphus fraxineus in Fraxinus excelsior. Phytopathol 106:1535–1543. https://doi.org/10.1094/PHYTO-11-15-0284-R

Myking T (2002) Evaluating genetic resources of forest trees by means of life history traits—a Norwegian example. Biodivers Conserv 11:1681–1696

Nemesio-Gorriz M, Menezes RC, Paetz C, Hammerbacher A, Steenackers M, Schamp K, Höfte M, Svatos A, Gershenzon J, Douglas GC (2020) Canditate metabolites for ash dieback tolerance in *Fraxinus excelsior*. J Exp Bot 71:6074–6083. https://doi.org/10.1093/jxb/eraa306

Nielsen LR, McKinney LV, Hietala AM, Kjær ED (2017) The susceptibility of Asian, European and North American *Fraxinus* species to the ash dieback pathogen *Hymenoscyphus fraxineus* reflects their phylogenetic history. Eur J Forest Res 136:59–73. https://doi.org/10.1007/s10342-016-1009-0

Nielsen LR, Nagy NE, Piqueras S, Kosawang C, Thygesen LG, Hietala AM (2022) Host–pathogen interactions in leaf petioles of common ash and Manchurian ash infected with *Hymenoscyphus fraxineus*. Microorganisms 10:375. https://doi.org/10.3390/microorganisms10020375

Norelli JL, Farrell RE, Bassett CL, Baldo AM, Lalli DA, Aldwinckle HS, Wisniewski ME (2009) Rapid transcriptional response of apple to fire blight disease revealed by cDNA suppression subtractive hybridization analysis. Tree Genet Genomes 5:27–40. https://doi.org/10.1007/s11295-008-0164-y

Pautasso M, Aas G, Queloz V, Holdenrieder O (2013) European ash (*Fraxinus excelsior*) dieback—a conservation biology challenge. Biol Conserv 158:37–49. https://doi.org/10.1016/j.biocon.2012.08.026

Pratt (2017) Management and use of Ash in Britain from the prehistoric to the present: some implications for its preservation. In: Vasaitis R, Enderle R (eds) Dieback of European Ash (Fraxinus spp.): Consequences and Guidelines for Sustainable Management 1–14

Qazi S, Lombardo D, Abou-Zaid M (2018) A metabolomic and HPLC-MS/MS analysis of the foliar phenolics, flavonoids and coumarins of the *Fraxinus* species resistant and susceptible to emerald ash borer. Molecules 23:2734. https://doi.org/10.3390/molecules23112734

R Core Team (2022) R: a language and environment for statistical computing. R Foundation for Statistical Computing, Vienna, Austria. https://www.R-project.org/

Ramsfield TD, Bentz BJ, Faccoli M, Jactel H, Brockerhoff EG (2016) Forest health in a changing world: effects of globalization and climate change on forest insect and pathogen impacts. Forestry 89(3):245–252. https://doi.org/10.1093/forestry/cpw018Ridley

Ridley M, Demir Ö, Charria-Girón E, Schulz B, Surup F, Steinert M, Enderle R (2024) Priming of ash saplings with a low virulent Hymenoscyphus fraxineus strain as a possible disease control approach for reducing symptoms of ash dieback. Research Square. https://doi.org/10.21203/rs.3.rs-4348277/v1

Sahraei SE, Cleary M, Stenlid J, Durling MB, Elfstrand M (2020) Transcriptional responses in developing lesions of European common ash (*Fraxinus excelsior*) reveal genes responding to infection by *Hymenoscyphus fraxineus*. BMC Plant Biol 20:455. https://doi.org/10.1186/s12870-020-02656-1

Sambles CM, Salmon DL, Florance H, Howard TP, Smirnoff N, Nielsen LR, McKinney LV, Kjær ED, Buggs RJ, Studholme DJ, Grant M (2017) Ash leaf metabolomes reveal differences between trees tolerant and susceptible to ash dieback disease. Sci Data 4:170190. https://doi.org/10.1038/sdata.2017.190

Schlegel M, Dubach V, Buol L, Sieber TN (2016) Effects of endophytic fungi on the ash dieback pathogen. FEMS Microbiol Eco 92:fiw142. https://doi.org/10.1093/femsec/fiw142

Schwanda K, Kirisits T (2016) Pathogenicity of *Hymenoscyphus fraxineus* towards leaves of three European ash species: *Fraxinus excelsior, F. angustifolia* and *F. ornus*. Plant Pathol J 65:1071–1083. https://doi.org/10.1111/ppa.12499

Simler-Williamson AB, Rizzo DM, Cobb RC (2019) Interacting effects of global change on forest pest and pathogen dynamics. Annu Rev Ecol Evol Syst 50:381–403. https://doi.org/10.1146/annurev-ecolsys-110218-024934

Sollars ESA, Harper AL, Kelly LJ et al (2017) Genome sequence and genetic diversity of European ash trees. Nature 541:212–216. https://doi.org/10.1038/nature20786

Stegmann M, Anderson RG, Ichimura K, Pecenkova T, Reuter P, Žárský V, McDowell JM, Shirasu K, Trujillo M (2012) The ubiquitin ligase PUB22 targets a subunit of the exocyst complex required for PAMP-triggered responses in *Arabidopsis*. Plant Cell 24:4703–4716. https://doi.org/10.1105/tpc.112.104463

Thompson ID, Okabe K, Tylianakis JM, Kumar P, Brockerhoff EG, Schellhorn NA, Parrotta JA, Nasi R (2011) Forest biodiversity and the delivery of ecosystem goods and services: translating science into policy. Bioscience 61:972–981. https://doi.org/10.1525/bio.2011.61.12.7

Timmermann V, Børja I, Hietala AM, Kirisitie T, Solheim H (2011) Ash dieback: pathogen spread and diurnal patterns of ascospore dispersal, with special emphasis on Norway. EPPO Bull 41:14–20. https://doi.org/10.1111/j.1365-2338.2010.02429.x

Van Moerkercke A, Steensma P, Schweizer F, Goossens A (2015) The bHLH transcription factor BIS1 controls the iridoid branch of the monoterpenoid indole alkaloid pathway in *Catharanthus roseus*. Proc Natl Acad Sci USA 112:8130–8135. https://doi.org/10.1073/pnas.1504951112

Wang Z, Gerstein M, Snyder M (2009) RNA-Seq: a revolutionary tool for transcriptomics. Nat Rev Genet 10:57–63. https://doi.org/10.1038/nrg2484

Yang T, Liu J, Li X, Amanullah S, Lu X, Zhang N, Zhang Y, Luan F, Liu H, Wang X (2022) Transcriptomic analysis of *Fusarium oxysporum* stress-induced pathosystem and screening of Fom-2 interaction factors in contrasted melon plants. Front Plant Sci 13:961586. https://doi.org/10.3389/fpls.2022.961586

Yoo AB, Jette MA, Grondona M (2003) SLURM: simple linux utility for resource management. In: Feitelson D, Rudolph L, Schwiegelshohn U (eds) Job scheduling strategies for parallel processing. JSSPP 2003. Lecture notes in computer science, vol 2862. Springer, Berlin, Heidelberg. https://doi.org/10.1007/10968987_3

You Q, Zhai K, Yang D et al (2016) An E3 ubiquitin ligase-BAG protein module controls plant innate immunity and broad-spectrum disease resistance. Cell Host Microbe 20(6):758–769. https://doi.org/10.1016/j.chom.2016.10.023

Yuan M, Ngou BPM, Ding P, Xin X-F (2021) PTI-ETI crosstalk: an integrative view of plant immunity. Curr Opin Plant Biol 62:102030. https://doi.org/10.1016/j.pbi.2021.102030

Zamora-Ballesteros C, Pinto G, Amaral J, Valledor L, Alves A, Diez JJ, Martin-Garcia J (2021) Dual RNA-Sequencing analysis of resistant (*Pinus pinea*) and susceptible (*Pinus radiata*) hosts during *Fusarium circinatum* challenge. Int J Mol Sci 22:5231. https://doi.org/10.3390/ijms22105231

Zaynab M, Fatima M, Abbas S, Sharif Y, Umair M, Zafar MH, Bahadar K (2018) Role of secondary metabolites in plant defense against pathogens. Microb Pathog 124:198–202. https://doi.org/10.1016/j.micpath.2018.08.034

Zeilmaker T, Ludwig NR, Elberse J, Seidl MF, Berke L, Doorn AV, Schuurink RC, Snel B, Ackerveken GV (2015) Downy mildew resistant 6 and DMR6-like oxygenase 1 are partially redundant but distinct suppressors of immunity in Arabidopsis. Plant J 81:210–222. https://doi.org/10.1111/tpj.12719